ORAL/POSTER REFERENCE: ICF100647

THE ROLE OF PARTICLES IN FATIGUE CRACK PROPAGATION OF ALUMINUM ALLOYS

Z.Z.Chen[1], K.Tokaji[2] and T.Horimoto[1]

[1] Graduate Student, Gifu University, 1-1 Yanagido, Gifu 501-1193, Japan
[2] Department of Mechanical and Systems Engineering, Faculty of Engineering, Gifu University, 1-1 Yanagido, Gifu 501-1193, Japan

ABSTRACT

Fatigue crack propagation (FCP) in two aluminum alloys (casting alloy, AC4CH, and aluminum alloy, A2024, reinforced with 5 μ m SiC particulates) was studied to understand the role of SiC and Si particles. In the SiC_P/Al composite, there were few particles appeared on the fracture surfaces even at high ΔK region, indicating that cracks propagated predominantly within the matrix avoiding SiC particles because of the high strength of the particles and the strong particle/matrix interface. In the casting alloy, Si particle debonding was more prominent. When compared with the SiC_P/Al composite, the casting alloy exhibited lower FCP rates, but had a slight steeper slope in the Paris region. Crack deflection and branching were found to be more remarkable in the casting alloy than in the SiC_P/Al composite that may contribute to better FCP resistance in the former alloy.

KEYWORDS: Aluminum matrix composite, Casting alloy, Fatigue crack propagation, Particle

INTRODUCTION

Aluminum-based matrix composites reinforced with silicon carbide particulates (MMCs) have received more attention in the past decade because the conventional metallurgical and machining processing techniques, such as direct casting, powder metallurgy, rolling, forging, and extrusion can be applied for their fabrication. Although the second phase additions can cause reduced tensile ductility, lower fracture toughness, and in some cases, decreased fatigue resistance compared with the constituent matrix alloy, SiC_P/Al composites still have potential in structural applications because of considerable weight saving due to their specific properties. On the other hand, the outstanding mechanical, physical, and casting properties of Al-Si-Mg alloys make them attractive for use in cheaper and lighter engineering components. The eutectic Si particles in Al-Si-Mg alloys can be considered as a reinforcement whose size, distribution and volume fraction may affect strongly

fatigue properties just like SiC particulates in SiC_P/Al composites. Some studies have been done to understand the effects of SiC and Si particles on fatigue resistance and fatigue crack propagation (FCP) in SiC_P/Al composites and in Al-Si-Mg casting alloys [1-6], but further studies are still needed to clarify the role of SiC and Si particles in FCP.

In the present study, FCP tests were conducted on casting alloy, AC4CH, and SiC_P/Al composite, and the role of SiC and Si particles in FCP and the mechanisms are discussed on the basis of detailed fractographic examination.

EXPERIMENTAL PROCEDURES

Materials

The materials used are aluminum casting alloy, AC4CH, and aluminum alloy 2024 reinforced with 10wt.% SiC particulates, the average particle size of 5μm, hereafter denoted as SiC_P/Al. The SiC_P/Al composite is fabricated by powder metallurgy. The chemical compositions (wt.%) are; Si 6.67, Mg 0.36, Fe 0.07, Ti 0.13, Sb 0.10, balance Al for the casting alloy, and Si 0.13, Fe 0.24, Cu 4.57, Mn 0.63, Mg 1.65, Cr 0.01, Zn 0.091, Ti 0.02, balance Al for the SiC_P/Al composite. The mechanical properties are listed in Table 1. The SiC_P/Al composite exhibits higher 0.2% proof stress, tensile strength and Young's modulus and lower elongation and reduction of area than the casting alloy. Figure 1 shows the microstructures. It can be seen that SiC particulates are well-distributed and tend to be weakly aligned to the extrusion direction (Figure 1(a)), while eutectic Si particles distribute to form dendrite cells (Figure 1(b)).

TABLE 1
MECHANICAL PROPERTIES OF ALLOYS

Alloy	Tensile strength (MPa)	0.2% proof stress (MPa)	Elongation (%)	Reduction of area (%)	Elastic modulus (GPa)
AC4CH	289	235	7	24	64
SiC_p/Al	462	365	5	8	71

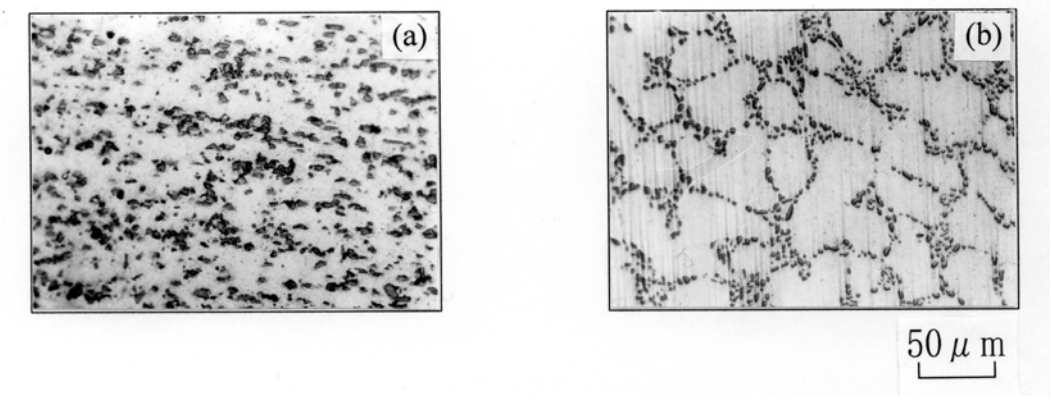

Figure 1: Microstructures: (a) SiC_P/Al, (b) AC4CH.

Test Methods

The casting alloy was solution treated at 530℃ for 6hrs followed by aging at 160℃ for 6hrs. The SiC_P/Al composite was also solution treated at 495℃ for 1h, quenched in water and then aged at 190℃ for 5hrs. CT specimens (W=24mm, B=5mm) were prepared after heat treatment. Experiments were conducted on an electro-servohydraulic fatigue testing machine operating at a frequency of 10Hz under load control with sinusoidal wave form in laboratory air at ambient temperature. Stress ratios were 0.05 and 0.7. Crack length was measured by a traveling microscope and crack closure was monitored by a compliance method using a strain gauge mounted on the back of the specimens. In the near threshold region, load shedding technique was employed to gradually decrease the FCP rate while keeping the stress ratio constant. In the region of $da/dN > 10^{-8}$ m/cycle, constant load amplitude tests were used. The da/dN and ΔK curves were obtained using a five points polynomial method. Crack path and fracture surfaces were examined using optical microscope and scanning electron microscope (SEM), respectively.

RESULTS AND DISCUSSION

FCP rate

Figure 2(a) and (b) show the relationships between da/dN and ΔK at R=0.05 and R=0.7 in both alloys, respectively. In Figure 2(a), the casting alloy exhibits a better FCP resistance than the SiC_P/Al composite and has a higher threshold value of approximately 5.2MPam$^{1/2}$ compared with 4.5MPam$^{1/2}$ in the SiC_P/Al composite. In $da/dN > 10^{-8}$m/cycle, the da/dN-ΔK relationships of both alloys can be expressed by the Paris law, while the casting alloy shows a slightly higher slope and the parameters of the Paris law, C and m, are 1.22×10^{-14} and 6.46 for the casting alloy and 6.64×10^{-12} and 4.24 in the SiC_P/Al composite, respectively. As can be seen in Figure 2(b), the FCP rates of both alloys are the same. Since crack closure was not recognized at R=0.7, the observed differences in FCP rate between both alloys in Figure 2(a) may be attributed to crack closure.

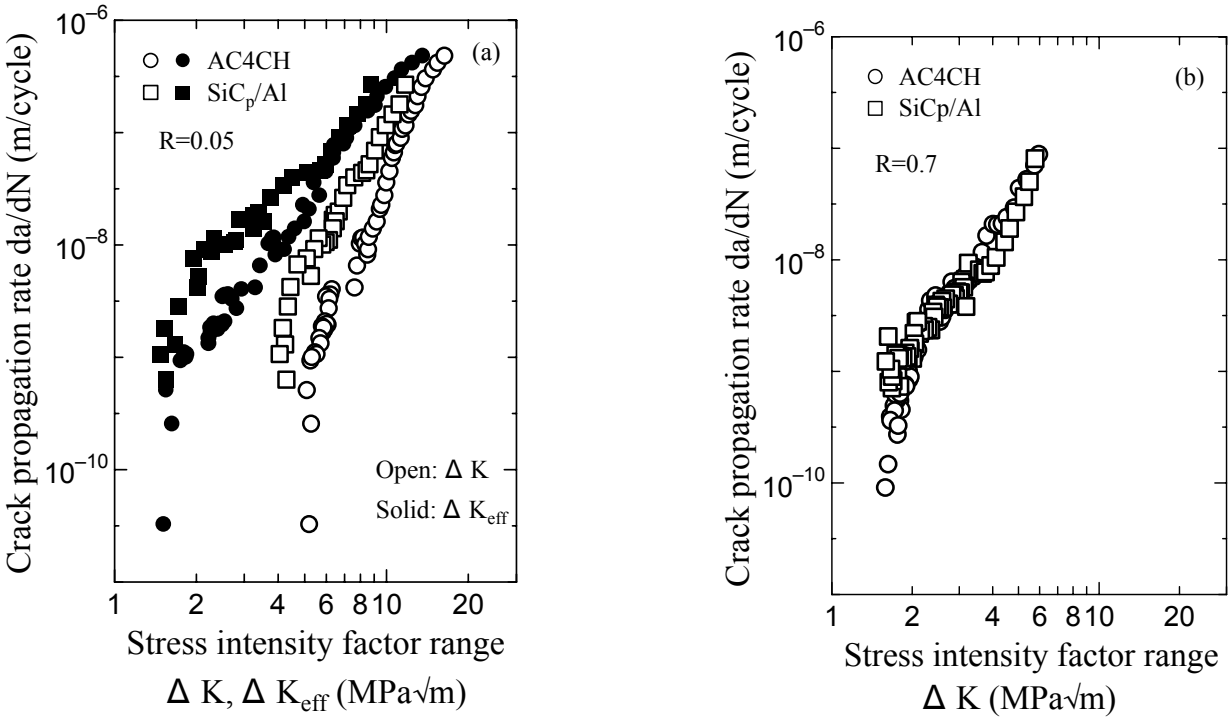

Figure 2: Relationships between da/dN and ΔK: (a)R=0.05, (b)R=0.7.

Crack closure behavior, K_{op}/K_{max}, is shown in Figure 3 as a function of K_{max}. It can be seen that the casting alloy shows higher closure levels than the SiC_p/Al composite in the intermediate K_{max} region, but the closure levels in both alloys are almost identical at high and low K_{max} regions. After allowing for crack closure, *i.e.* in terms of the effective stress intensity factor range, ΔK_{eff}, there exist still differences in FCP rate between both alloys (see Figure 2(a)), but it should be noticed that the threshold value is nearly the same. Comparison between Figure 2(a) and (b), the da/dN- ΔK relationship at R=0.7 in the casting alloy is consistent with the da/dN- ΔK_{eff} relationship at R=0.05, while the differences in FCP rate between both can be seen in the SiCp/Al composite.

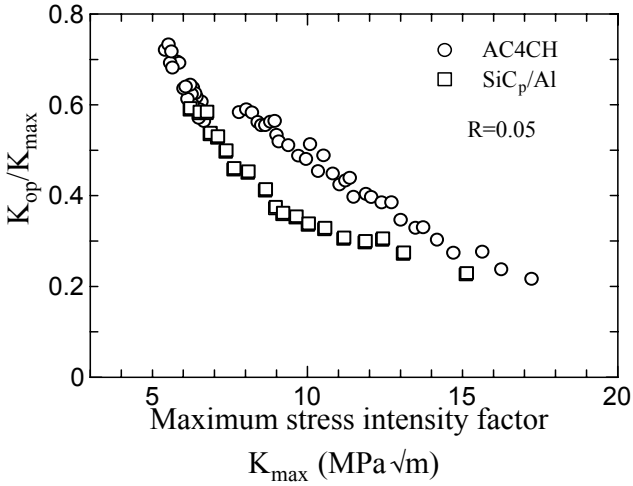

Figure 3: Crack closure behavior.

Crack path profile

Figure 4 reveals the crack paths at different FCP rates, *i.e.* ΔK levels, in both alloys. The crack paths of the SiC_P/Al composite are rather smooth regardless of ΔK. On the contrary, the casting alloy exhibits remarkable crack deflections and the crack paths are much more tortuous compared with the SiC_P/Al composite. As ΔK increases, the fracture surface roughness decreases. Therefore, the better FCP resistance in the casting alloy may be attributed to crack deflection *i.e.* fracture surface roughness, because of the higher crack closure levels and the reduction in the actual crack driving force at the crack tip [7]. Branching and bridging due to particle debonding can also be seen in the casting alloy, which can contribute to higher FCP

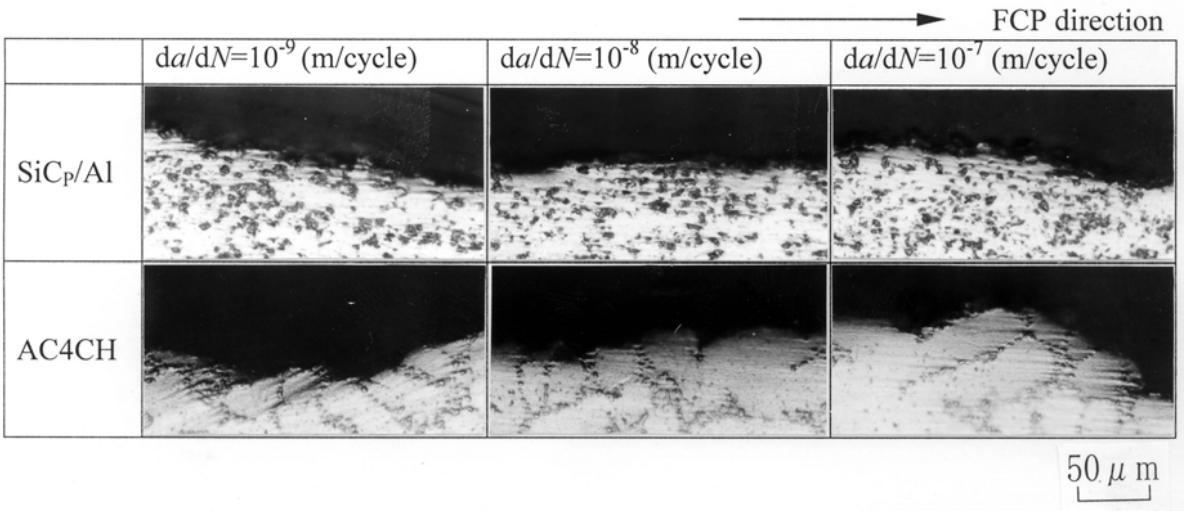

Figure 4: Optical micrographs of crack path profiles in SiC_P/Al and AC4CH.

resistance. Furthermore, there exist a lot of porosity defects in the casting alloy that enhance FCP rate by coalescence/linkage of those defects. Contrarily, those defects may also cause crack deflections that can promote crack closure, in turn leading to decreased FCP rate.

Fractographic analysis of fracture surfaces

SEM micrographs of fracture surfaces of the SiC_P/Al composite and the casting alloy are shown in Figure 5. In the SiC_P/Al composite, the main features are hills and concavities that are caused when cracks propagate enveloping or avoiding SiC particles. Exposure of bare SiC particles on the fracture surfaces is very rare, indicating a good interfacial bond between SiC particle and matrix. However, debonded coarse SiC particles can be seen occasionally, particularly in high ΔK region. Around debonded coarse SiC particles, secondary crackings can be seen that may be the result of the thin matrix layer's enveloping SiC particles being torn. In the casting alloy, the facet is main feature on fracture surface at low ΔK region, while the secondary crackings can be observed at intermediate and high ΔK regions. Debonded eutectic Si particles are clearly seen, especially in low ΔK region and the debonded Si particles along the dendrite cells are just like that observed in Figure 1, suggesting that cracks propagated along the boundaries of dendrite cells. Few fractured Si particles are observed even at high ΔK regions. Decohesion of Si particles from the surrounding matrix is the main mode of fracture in this case. It should be noticed that eutectic Si particles appeared on the fracture surfaces tend to decrease as ΔK increases, *i.e.* FCP rate increases. This implies that cracks often grow in the matrix at high ΔK region, leading to smoother crack paths, as shown in Figure 4.

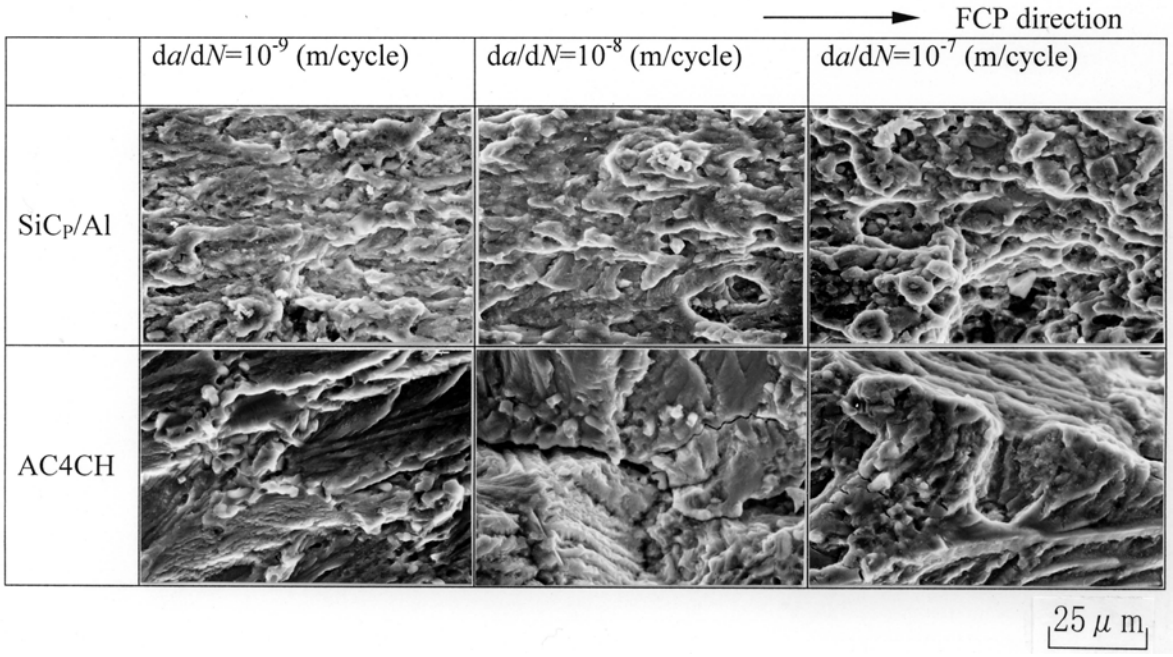

Figure 5: SEM micrographs of fracture surfaces in SiC_P/Al and AC4CH.

Crack growth mechanisms

In the SiC_P/Al composite, cracks grow preferably in the matrix avoiding SiC particles regardless of ΔK, because of a good interfacial bond between SiC particles and matrix and high strength of SiC particles. The particle size is small, thus the fracture surfaces become smooth. On the contrary, in the casting alloy, cracks propagate along the dendrite cells due to the debonding of Si particles in low ΔK region. In this case, there are two factors that may affect crack propagation; the first is that the cluster distribution causes the Si particles debonding easier and the second is that the Si particles along the dendrite cells may act as an "egg-shell" [4]. In the latter, cracks will need extra stress to advance into the next dendrite cell compared with propagating along the boundaries of dendrite cells. Whether cracks propagate along or through the

dendrite cells depend strongly on the crack-tip driving force and the strength of "egg-shell". In low ΔK region, cracks prefer to propagating along the boundaries of dendrite cells because Si particles provide a weak path, while in high ΔK region, cracks can break the "egg-shell" and thus grow into the inside of the next dendrite cell.

CONCLUSIONS

FCP tests were conducted on casting alloy, AC4CH, and SiC_P/Al composite, and the role of SiC and Si particles in FCP and the mechanisms are discussed on the basis of detailed fractographic examination.

1. Both alloys showed considerable differences in FCP behavior that was mainly attributed to the difference in particle distribution.
2. The casting alloy showed lower FCP rates compared with the SiC_p/Al composite, but had a slightly steeper slope in the Paris region.
3. After allowing for crack closure or in the crack closure-free FCP behavior, there were no significant differences in FCP rate between both alloys, indicating that the higher FCP resistance in the casting alloy was attributed to crack closure.
4. In the SiC_P/Al composite, cracks propagated avoiding SiC particles and predominantly within the matrix, while in the casting alloy, debonding of eutectic Si particles was the main feature and cracks grew to link debonded particles along dendrite cells that caused remarkable crack deflections.

REFERENCES

1. CHITOSHI MASUDA, YOSIHISA TANAKA, *etc*. (1994) *Adv. Composite Mater.* **3 No.4**, 319.
2. F.T. LEE, J.F. MAJOR, and F.H. SAMUEL. (1995) *Fatigue Fract. Engng Mater. Struct.* **18 No.3**, 385.
3. S. Kumai, K Yoshida, Y. Higo and S. Nunomura. (1992) *Int. J Fatigue,* **14 No.2**, 105.
4. ZHIRUI WANG and RUBY J. ZHANG. (1994) *Acta metal. Mater.* **42**, 1433
5. O.BOTSTEIN, R.ARONE and B.SHPIGLER. (1990) *Mater. Sci. Eng.* **A128,** 15.
6. KEN GALL, NANCY YANG, *etc*. (1999) *Metal. Mater. Trans.* **30A**, 3079.
7. S. SURESH. (1983) *Metal. Trans. A* **14A**, 2375.